# Pseudo-vacuum magnetic boundary condition. Numerical benchmark.

**Andrei Sheyko.**

July 10, 2012

## Contents

## Introduction

Here we present a benchmark study for the convection-driven magnetohydrodynamic dynamo problem in a rotation spherical shell with "pseudo-vacuum" magnetic boundary condition.

## 1 MHD equations

The chosen form of the non-dimensionalised magnetohydrodynamic equations is:

$$\begin{cases} \left(Ro\,\dfrac{\partial}{\partial t} - E\boldsymbol{\nabla}^2\right)\vec{u} &= Ro\,\vec{u}\times(\boldsymbol{\nabla}\times\vec{u}) + (\boldsymbol{\nabla}\times\vec{B})\times\vec{B} + q\,Ra\,T\,\vec{r} - \hat{\vec{z}}\times\vec{u} - \boldsymbol{\nabla}\hat{P}, \\ \left(\dfrac{\partial}{\partial t} - \boldsymbol{\nabla}^2\right)\vec{B} &= \boldsymbol{\nabla}\times(\vec{u}\times\vec{B}), \\ \left(\dfrac{\partial}{\partial t} - q\boldsymbol{\nabla}^2\right)T &= -\vec{u}\cdot\boldsymbol{\nabla}T, \end{cases} \tag{1}$$

$$\boldsymbol{\nabla}\cdot\vec{B} = 0,\ \boldsymbol{\nabla}\cdot\vec{u} = 0 \tag{2}$$

$$\text{Length } r \to (d = r_o - r_i)\,r, \quad \text{Time } t \to d^2/\eta\,t, \quad \text{Magnetic } B \to (2\Omega\rho_0\mu_0\eta)^{\frac{1}{2}}\,B, \quad \text{Temperature } T \to \Delta T\,T \tag{3}$$

with dimensionless parameters:

$$\begin{array}{rr} \text{Magnetic Rossby number} & Ro = \eta/(2\Omega d^2), \\ \text{Ekman number} & E = \nu/(2\Omega d^2), \\ \text{Modified Rayleigh number} & Ra = \dfrac{g\,\alpha\,\Delta T\,d}{2\Omega\kappa}, \\ \text{Roberts number} & q = \kappa/\eta. \end{array} \tag{4}$$

Ratio $r_o/r_i = 0.35$ in used for simulations in this report. Together with the definition of the unit length $d$ it gives $r_i = 7/13$, $r_o = 20/13$.

## 2 Boundary and initial conditions

### 2.1 Magnetic boundary condition

The form of the magnetic boundary condition is:

$$B_\theta = B_\phi = 0|_{r_i,r_o}\,, \tag{5}$$

$r_i$ and $r_o$ denote inner and outer radii of the spherical shell. This represents equating of the tangential to the spherical boundary surface component of the magnetic field to zero. Physically it means that the radial component of the current on boundaries is zero ( $\left.\left(\boldsymbol{\nabla}\times\vec{B}\right)_r\right|_{r_i,r_o} = 0$ ). The locality of this condition is an advantage in finite difference numerical schemas.

The condition on $B_r$ can be extracted from the differential form of the Gauss's law for magnetism:

$$\boldsymbol{\nabla}\cdot\vec{B} = 0. \tag{6}$$

If tangential components of the field are zero (eq.(5)), this law in spherical coordinates contains only radial component of the field:

$$\frac{\partial}{\partial r}(r^2 B_r) = 0|_{r_i,r_o}, \tag{7}$$

or simply:

$$\left(2 + r\frac{\partial}{\partial r}\right)B_r = 0|_{r_i,r_o}. \tag{8}$$

## 2.2 Initial magnetic field

The initial magnetic field is:

$$\begin{aligned}
B_r &= \frac{1}{\sqrt{2}}\frac{5}{8}\frac{-48\,r_i\,r_o + (4\,r_o + r_i\,(4+3\,r_o))\,6r - 4(4+3\,(r_i+r_o))\,r^2 + 9\,r^3}{r}\cos\theta, \\
B_\theta &= -\frac{1}{\sqrt{2}}\frac{15}{4}\frac{(r-r_i)\,(r-r_o)\,(3\,r-4)}{r}\sin\theta, \\
B_\phi &= \frac{1}{\sqrt{2}}\frac{15}{8}\sin\pi(r-r_i)\sin 2\theta.
\end{aligned} \tag{9}$$

It is easy to see that $B_\theta = B_\phi = 0$ at $r_i$ and $r_o$, the condition $\frac{\partial}{\partial r}(r^2 B_r) = 0|_{r_i,r_o}$ is satisfied as well (see eq.(7)).

Figure 1: Initial magnetic field, meridional slices

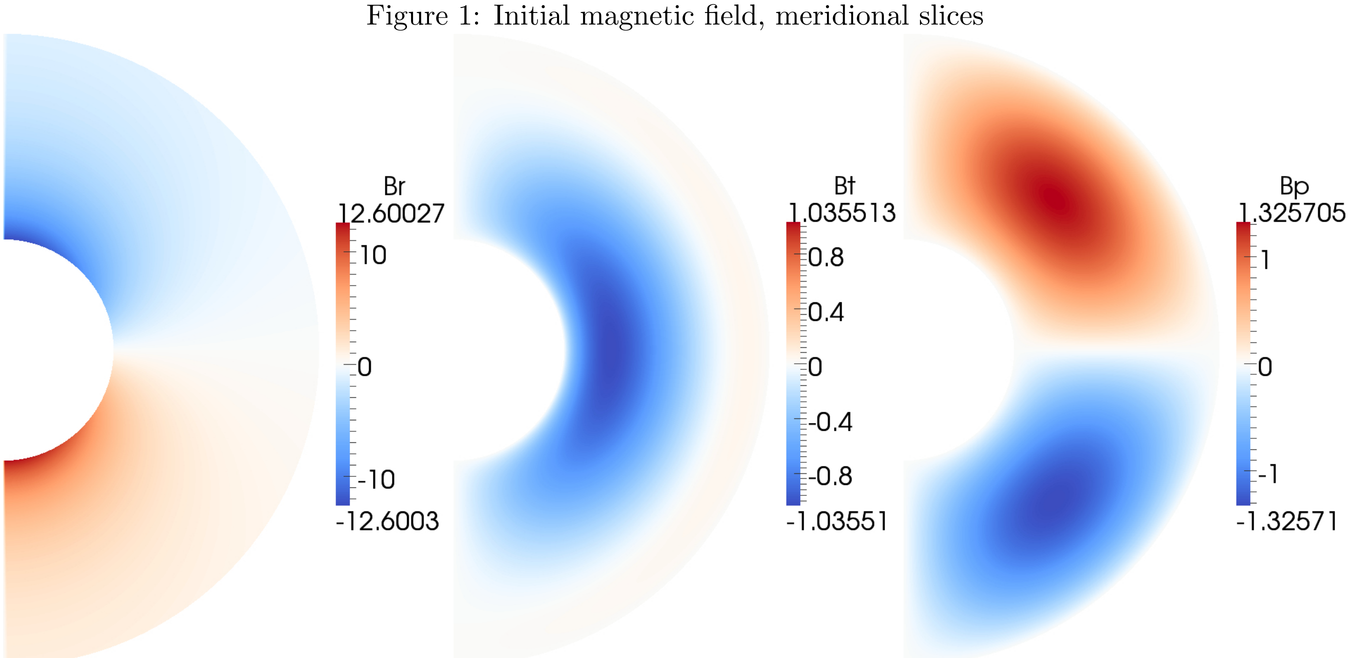


## 2.3 Initial temperature field and boundary conditions

Initial temperature is the same as in Christensen et al. (2001)

$$T = \frac{r_o r_i}{r} - r_i + \frac{21}{\sqrt{17920\pi}}(1 - 3x^2 + 3x^4 - x^6)\sin^4\theta\cos 4\varphi, \tag{10}$$

where $x = 2r - r_i - r_o$. This describes a conductive state with a perturbation of harmonic degree and order four super-imposed.

Temperature is fixed on boundaries : $T(r_i) = 1$, $T(r_o) = 0$.

Figure 2: Initial temperature, equatorial and meridional slices

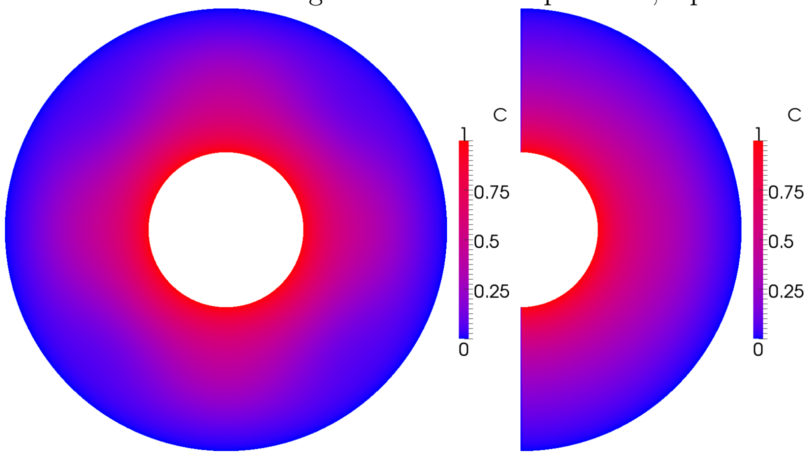


### 2.4 Initial velocity field and boundary conditions

Initial velocity is zero. No-slip and non-penetrating boundary conditions are imposed.

## 3 Numerical method

Spherical harmonic expansion on spherical surfaces(L degrees and M orders), finite differences in the radial direction(N-points on Chebyshev grid), adaptive predictor-corrector semi-implicit time-stepping algorithm are used.

## 4 The benchmark study

In this section we describe steady (where the magnetic energy is constant in time) dynamo which can be suitable for a benchmark study. Parameters are suggested by Harder and Hansen (2005).

The solution has fourfold symmetry in longitude and is symmetric about equator. In one of the calculations fourfold symmetry was used to restrict spherical harmonics expansion and accordingly the computer time (the run with the lowest resolution 50/32/29, see table (1)).

In order to compare results obtained at different resolutions and control convergence, resolution is defined as the third root of the number of degrees of freedom for each scalar variable:

$$R = N^{1/3}\,(L\,(2M+1) - M^2 + M + 1)^{1/3}. \tag{11}$$

### 4.1 Requested data

Global averages and local data at specific points are requested from the simulations.
**Global data.**
The solution can be expressed in the form $(\vec{u}, \vec{B}, T) = f(r, \theta, \varphi - \omega\, t)$. Angular speed $\omega$, magnetic and kinetic energies, which are defined as:

$$E_{mag} = \frac{1}{2\,Ro}\int B^2\, dV \tag{12}$$

$$E_{kin} = \frac{1}{2}\int u^2\, dV. \tag{13}$$

are requested.

**Local data.**

A point where local data are to be taken is fixed in the drifting reference frame. We take a point at a mid depth ($r = (r_i + r_o)/2$) in the equatorial plane ($\theta = \pi/2$) whose $\phi$-coordinate is given by the conditions $u_r = 0$ and $\dfrac{\partial u_r}{\partial \varphi} > 0$. For this point $u_\phi$, $B_\theta$ and $T$ are requested.

## 4.2 Results

Parameters are the same as in the Christensen et al. (2001) benchmark Case 1, in our non-dimensionalisation:

| $E$ | Ra | q | Ro |
|---|---|---|---|
| $0.5 \cdot 10^{-3}$ | 32.50 | 5 | $10^{-4}$ |

Results of the integration are on the figure (3). Requested data of the simulation are in the table (1). It is plotted on the figure (4). The run should be integrated long enough to obtain desired precision.

| N | L | M | $u_\varphi$ | $B_\theta$ | $T$ | $E_{mag}$ | $E_{kin}$ | $\omega$ | d$t$ |
|---|---|---|---|---|---|---|---|---|---|
| 50 | 32 | 29 | -58.0792 | 0.9860 | 0.4261 | 79849.4 | 14892.8 | 3.7656 | 1.6272e-05 |
| 80 | 42 | 42 | -58.1670 | 0.9931 | 0.4259 | 80076.3 | 14847.3 | 3.7510 | 1.5903e-05 |
| 96 | 48 | 48 | -58.1705 | 0.9935 | 0.4259 | 80076.2 | 14846.9 | 3.7489 | 1.6108e-05 |
| 96 | 60 | 53 | -58.1796 | 0.9929 | 0.4260 | 80074.7 | 14847.2 | 3.7490 | 1.5779e-05 |
| 128 | 64 | 64 | -58.1786 | 0.9930 | 0.4259 | 80072.7 | 14846.9 | 3.7489 | 1.5795e-05 |
| 200 | 100 | 100 | -58.1786 | 0.9930 | 0.4259 | 80072.7 | 14846.5 | 3.7488 | 1.5741e-05 |

Table 1: Requested data.

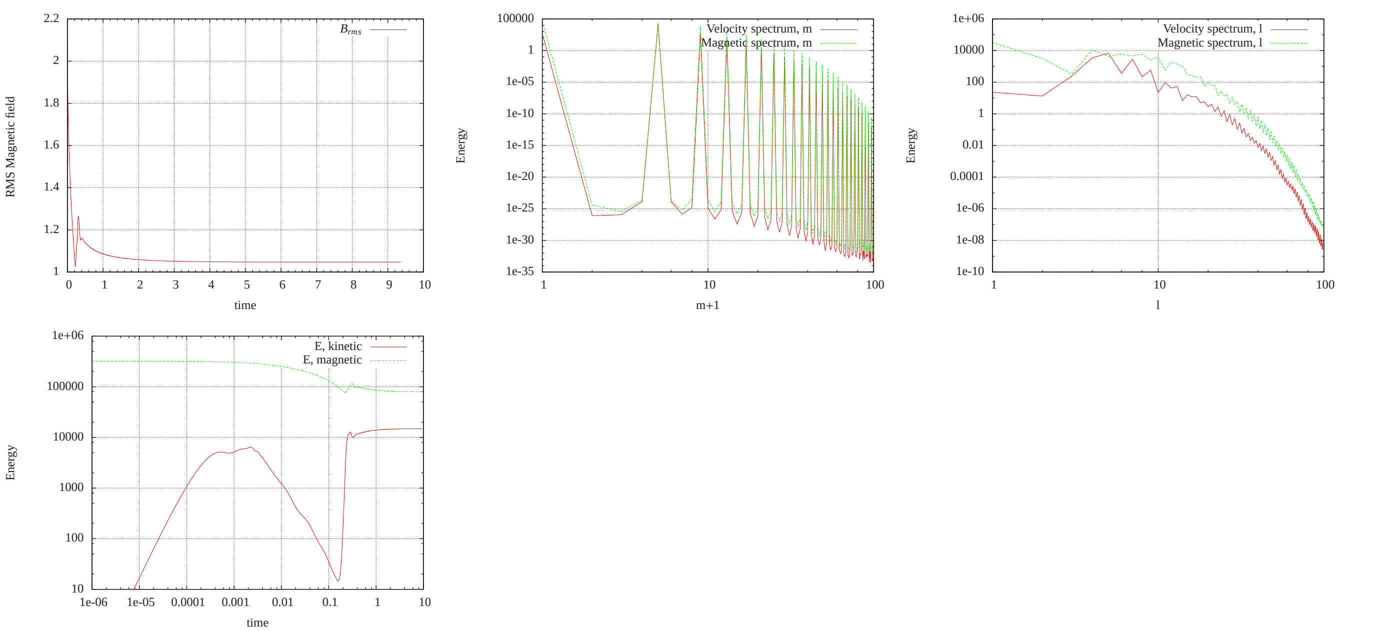


Figure 3: Diagnostics.

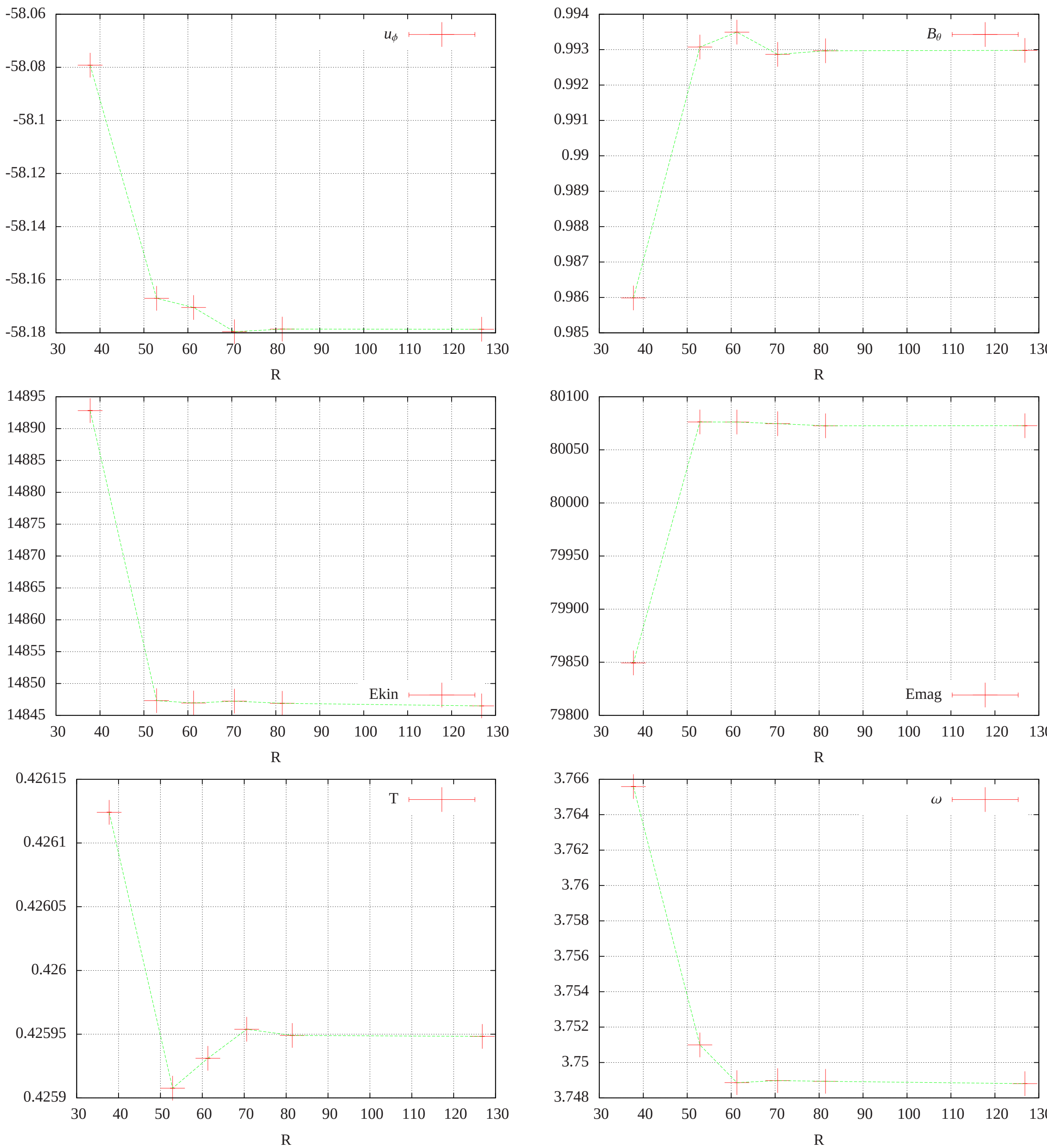


Figure 4: Resolution tests.

### 4.2.1 Field structure of the steady solution

The snapshot is taken in the region where the dynamo is steady. Meridional sections are in the plane of the benchmark point (defined in seq.(4.1)).

Meridional sections:

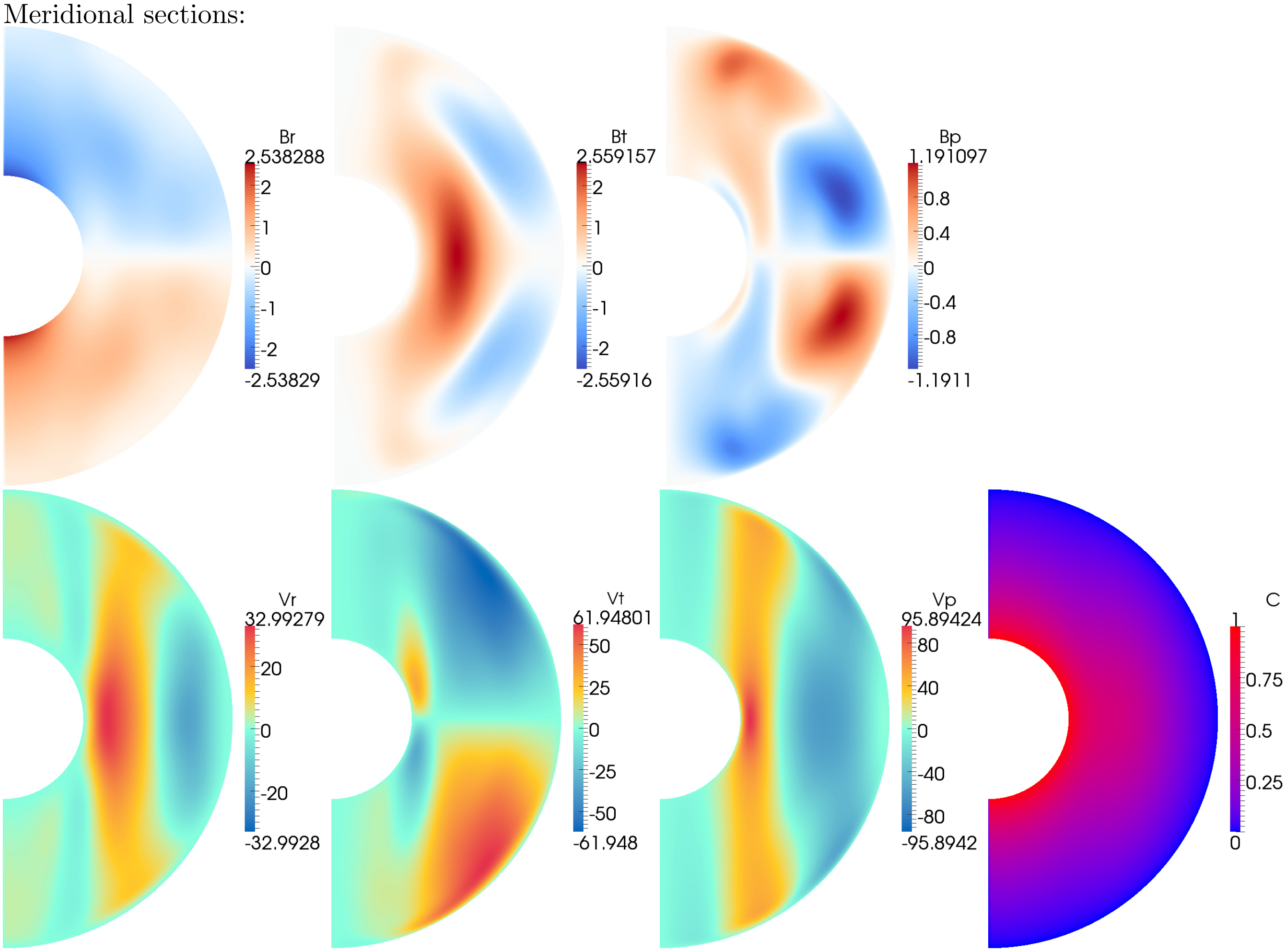


Equatorial sections:

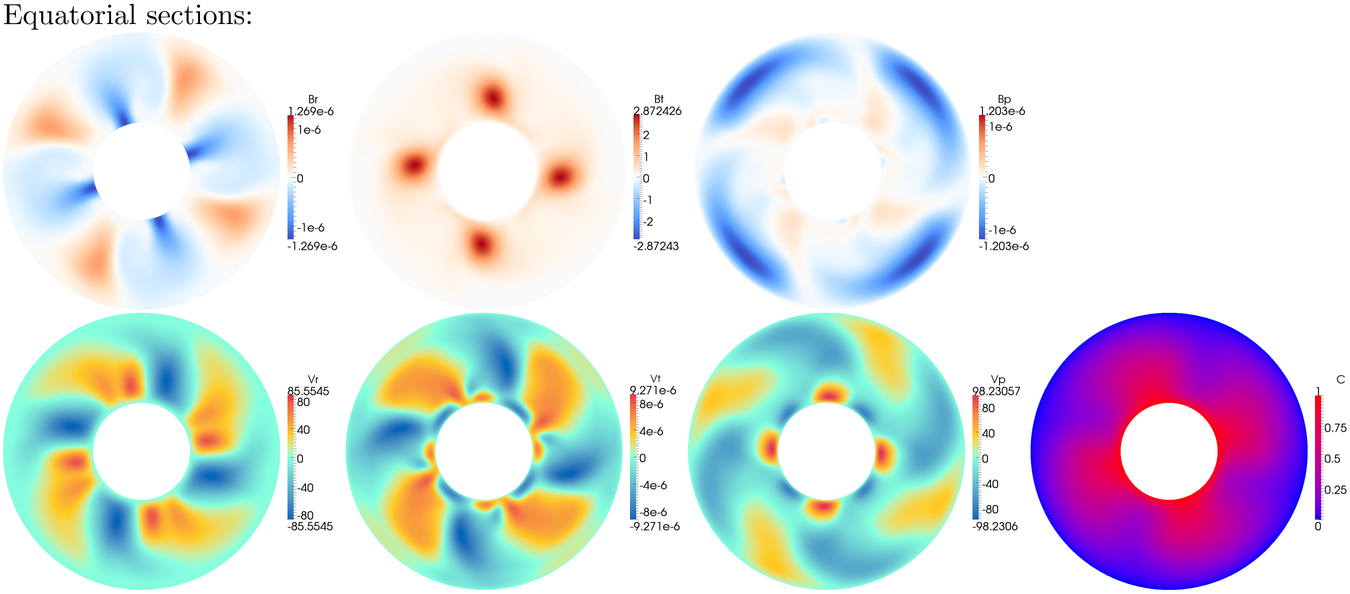

### 4.2.2 Timestep

Timestep is adaptive and in principle can change, but at the steady state it is almost constant. Dependence of the timestep on the resolution is on the fig.(5).

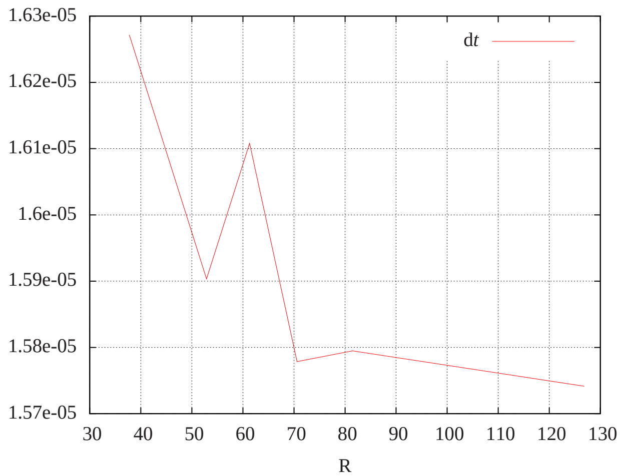


Figure 5: Timestep.

# 5 Conclusions

The steady drifting dynamo satisfying "pseudo-vacuum" magnetic boundary conditions together with the recipe to achieve it are presented. Due to the subcriticality the proper initial condition is required, the example of which is given in analytical form. The solution has fourfould and equatorial symmetries which can be useful to reduce cpu load during benchmarking.

Properties of dynamos obeying pseudo-vacuum and insulating boundary conditions are largely different. Comparison with the insulating case in Christensen et al. (2001) shows that the switch between the boundary conditions affects the direction and the speed of the drift, repartition of the kinetic and magnetic energies, geometry of fields.

# A Magnetic boundary condition in spectral form

Magnetic vector $\vec{B}$ can be written in terms of the toroidal and poloidal scalar fields, $T$ and $P$:

$$\vec{B} = \boldsymbol{\nabla} \times (T\vec{r}) + \boldsymbol{\nabla} \times \boldsymbol{\nabla} \times (P\vec{r}) \tag{14}$$

Projections of the magnetic field on the axes of the spherical coordinate system can be obtained directly from the scalar fields $P$ and $T$:

$$\begin{cases} B_r = -r\boldsymbol{\nabla}_1^2 P \\ B_\theta = \dfrac{1}{\sin\theta}\dfrac{\partial T}{\partial \phi} + \dfrac{1}{r}\dfrac{\partial}{\partial r}\left(r\dfrac{\partial P}{\partial \theta}\right) \\ B_\phi = -\dfrac{\partial T}{\partial \theta} + \dfrac{1}{r\sin\theta}\dfrac{\partial}{\partial r}\left(r\dfrac{\partial P}{\partial \phi}\right) \end{cases} \tag{15}$$

where

$$\boldsymbol{\nabla}_1^2 f = \frac{1}{r^2\sin\theta}\frac{\partial}{\partial\theta}\left(\sin\theta\frac{\partial f}{\partial\theta}\right) + \frac{1}{r^2\sin^2\theta}\frac{\partial^2 f}{\partial\phi^2} = -\frac{l(l+1)}{r^2} \tag{16}$$

Here we used the fact that the toroidal and poloidal scalars can be decomposed in spherical harmonics of the form:

$$\hat{Y}_l^m(\theta,\phi) = P_l^m(\cos\theta)e^{im\phi} \tag{17}$$

Boundary condition (5) with the use of equations (15) can be satisfied by keeping toroidal scalar $T = 0$ on boundaries and:

$$\frac{\partial(Pr)}{\partial r} = 0\bigg|_{r=r_i,r_o}. \tag{18}$$

The same equation, but expanded, is:

$$\left(\frac{\partial}{\partial r} + \frac{1}{r}\right)P = 0\bigg|_{r=r_i,r_o}. \tag{19}$$

# B Magnetic initial condition in spectral form

Spectral form of the initial magnetic field is:

$$\begin{cases} T_2^0 = \dfrac{1}{\sqrt{2}}\dfrac{5}{4}\sin\pi\,(r-r_i), \\ P_1^0 = \dfrac{1}{\sqrt{2}}\dfrac{5}{16}\left(-48\,r_i\,r_o + (4\,r_o + r_i\,(4+3\,r_o))\,6r - 4(4+3\,(r_i+r_o))\,r^2 + 9\,r^3\right). \end{cases} \tag{20}$$

# C Magnetic initial condition in the form of the vector potential

$$\begin{cases} A_r = \dfrac{1}{\sqrt{2}}\dfrac{15}{16}r\sin[\pi(r-r_i)]\cos(2\theta) + f_1(r) + \int (A_\theta(r,\theta) + r\dfrac{\partial A_\theta(r,\theta)}{\partial r})\mathrm{d}\theta \\ A_\theta = f_2(r,\theta) \\ A_\phi = \dfrac{1}{\sqrt{2}}\dfrac{5}{16}[-48r_ir_o + (4r_o + r_i(4+3r_o))6r - 4(4+3(r_i+r_o))r^2 + 9r^3]\sin\theta + K/(r\sin\theta) \end{cases}$$

where $\vec{B} = \boldsymbol{\nabla}\times\vec{A}$; $f_1$, $f_2$ are arbitrary functions; $K$ is an arbitrary constant.[1]

[1] Courtesy to David Cébron for this form of the initial field.

## References

Christensen, U.R., Aubert, J., Cardin, P., Dormy, E., Gibbons, S., Glatzmaier, G.A., Grote, E., Honkura, Y., Jones, C., Kone, M., Matsushima, M., Sakuraba, A., Takahashi, F., Tilgner, A., Wicht, J., and Zhang, K. A numerical dynamo benchmark. *Phys. Earth Planet. Interiors*, (128), 25–34, 2001.

Harder, Helmut and Hansen, Ulrich. A finite-volume solution method for thermal convection and dynamo problems in spherical shells. *Geophys. J. Int.*, (161), 522–532, 2005.